Nanoscale

Accepted Manuscript

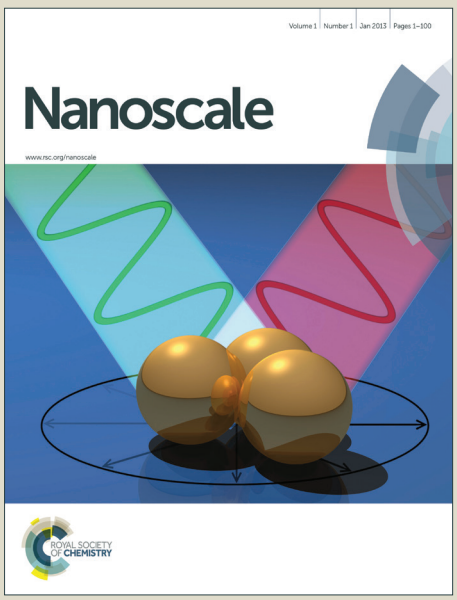

ROYAL SOCIETY OF CHEMISTRY

www.rsc.org/nanoscale

Journal Name

RSCPublishing

ARTICLE

Multiphoton excited coherent random laser in ZnO powders

Cite this: DOI: 10.1039/x0xx00000x

Christian Tolentino Dominguez*[a,c], Maria A. Gomes[b], Zélia S. Macedo[b], Cid B. de Araújo[c], and Anderson S. L. Gomes*[c]

Received 00th January 2012,
Accepted 00th January 2012

DOI: 10.1039/x0xx00000x

www.rsc.org/

We report the observation and analysis of anti-Stokes coherent random laser (RL) emission from zinc oxide (ZnO) powders excited by one-, two- or three-photons femtosecond laser radiation. The ZnO powders were produced using a novel proteic sol-gel low-cost and environment friendly material route that employs coconut water in the polymerization step of the metal precursor. One- and two-photon excitation at 354 nm and 710 nm, respectively, generated single band emissions centered at ≈ 387nm. For the three-photon excitation, the emission spectra showed a strong UV band (380-396 nm) attributed to direct three-photon absorption from the valence to the conduction band. The presence of an intensity threshold and a bandwidth narrowing of the UV band from ≈ 20 to ≈ 4 nm are clear evidences for RL action. Furthermore, the observation of multiple sub-nanometer narrow peaks in the emission spectra for excitation above the RL threshold is consistent with random lasing by coherent feedback.

Introduction

Random lasers (RLs) belong to a special class of lasers with optical feedback due to multiple light scattering in a disordered amplifying media.[1,2] As in a conventional laser, the RL action occurs when, for excitation above certain light intensity threshold, the optical gain of a luminescence transition is larger than the overall losses. First studied in 1966,[3] a turnover in this field occurred in 1994,[4] after the unambiguous experimental demonstration in which a dye-solution containing TiO_2 nanoparticles was employed for the observation of laser-like emission, latter named random laser. Since then, a myriad of multidisciplinary research succeeded exploiting strongly scattering disordered materials.[5,6] Besides colloidal systems with different size and shape of light scatterers,[7,8] RLs were observed for example in polymers,[9] photonic crystals infiltrated with a laser dye,[10] dye-doped polymer film/TiO_2-nanomembranes arrangement[11] and cold atoms.[12] Of great technological importance are the electrically excited RLs.[13-16] The question of coherent versus incoherent feedback from the scattering media was clarified[1,2,6] as well as the photon statistics.[17] The lack of directionality due to the multiple scattering nature of the feedback mechanism has been tackled in different ways. One alternative exploited surface plasmons excitation in a silver film.[18] Random fiber lasers have also been demonstrated[19-22] as well as a planar microcavity with random gain layers.[23] Another important aspect, lack of tunability, was mitigated in a number of ways. In one approach, single-particle resonances were cleverly exploited to provide resonant tunability.[24] Spatial profile and mode control have been exercised in a number of ways.[25,26]

All references mentioned above are based on one-photon excitation (1PE) for obtaining random lasing in the Stokes side of the excitation laser wavelength. Frequency upconversion (UC) RLs with anti-Stokes emission were also demonstrated with basis on two-photon absorption (2PA) processes in GaAs[27] and ZnO[28] powders. An energy transfer process was also exploited to obtain ultraviolet (UV) RL involving pairs of neodymium ions in a glass powder.[29] The anti-Stokes RLs also present low spatial and temporal coherence analogously to the down-converted RLs, but have the advantage that light in the UV may be obtained using an excitation laser operating in the visible or near-infrared range. In two recent reports, our group demonstrated three-photon excited random lasers in a dye/TiO_2 NPs colloid[30] and in a ZnO-on-Si nanostructured film.[31] In the first study,[30] a highly efficient dye, having a large three-photon absorption (3PA) cross section, was employed. Excitation at 1350 nm with femtosecond pulses generated visible coherent RL emission at ≈ 560 nm by direct 3PA. In the second study,[31] a ZnO nanostructured film was produced by a Plasma Immersion Ion Implantation and Deposition process, and by femtosecond excitation at 802 nm, direct three-photon band-to-band absorption generated RL emission at 390 nm. In this case, the film structure leads to a photon diffusion process in which interference contributes negligibly to the feedback mechanism, and as a consequence, this RL falls in the category of nonresonant or incoherent feedback.

In the present paper, we demonstrate that coherent upconverted RL emission due to direct 3PA in zinc oxide (ZnO) powders can be obtained by exciting at 802 nm with femtosecond pulses. This is the first time to our knowledge that an anti-Stokes coherent RL emission due to 3PA is observed in powders with grains that act simultaneously as scatterers and amplifiers. The three-photon excited RL operated in the UV region (380-396 nm) and the observation of narrow peaks in the emitted UV spectrum for excitation above the RL threshold is consistent with random lasing with coherent

feedback. We also characterized RL emission excited by one- and two-photon in the same sample for direct comparison.

Zinc oxide is one of the most important large bandgap semiconductors already being applied in different areas.[33] The versatility of ZnO arises from its 3.37 eV wide bandgap and its high excitonic binding energy of 60 meV. Among the diversity of applications, ZnO has been employed as field emitters, as front contact to solar cells, in liquid crystal displays and light emitting diodes;[34] biomedical application, such as antibacterial and antifungal properties of ZnO NPs, have also been demonstrated.[35] Furthermore, laser emission was demonstrated in different ZnO morphologies (sub-micrometer particles, thin films, urchin-like structures and bulk samples) and temporal excitation regimes (femtosecond to nanoseconds),[36-39] including one-photon excited RL.[1,2,40]

Experimental

The ZnO powders used in the present work were synthesized following a new green synthesis route exploiting a proteic sol-gel, in which filtered coconut water is employed in the polymerization step of metal precursors. In this route, the metal ions are believed to bind to the polymeric chains of proteins present in the coconut water, forming a colloidal suspension (sol).[41] The proteic sol-gel has the advantage of being a low cost, low toxic and simple methodology synthesis route and has been successfully used to produce metal oxide nanoparticles and thin films with fine control of size and agglomeration of the nanostructures.[42-44] In a typical procedure, zinc nitrate hexahydrated (Aldrich, PA) was firstly dissolved in distilled water. Subsequently, filtered coconut water was added into the nitrate solution under mild magnetic stirring for 30 min. The resulting sol was placed to dry at 100 °C for 24 hours and then pre-calcined at 200 °C for 5 hours, forming the precursor powder. With the precursor powder, a washing step with distilled water followed by centrifugation was employed to eliminate residual KCl salt derived from the coconut water. The washed precursor powder was finally calcined at 1000 °C for 5 hours. The morphology and crystallographic orientation of the ZnO grains were characterized by scanning electron microscopy (SEM) and X-ray diffraction.

Figure 1a shows a SEM image of the grains that have polyhedral shape with average dimensions of ≈ 600 nm. The crystalline structural phase was confirmed by X-ray diffraction as illustrated in Fig. 1b.

For the RL excitation a pulsed Ti: sapphire laser (802 nm, 100 fs, 1 kHz, pulse energy up to 1 mJ) or the output of an optical parametric amplifier (OPA) at 354 nm or 710 nm was used. The pulse duration and repetition rate followed the Ti: sapphire excitation source. A mass of 26.4 mg of ZnO powder was placed in a sample holder (dimensions: ≈ 7 x 1.1 x 1.1 mm^3) and a stripe excitation geometry was used with a cylindrical lens at an angle of 90 degrees with respect to the sample face (see the inset of Fig. 2a). The stripe dimensions were adjusted for the different wavelength used. For one-photon excitation (1PE) at λ_{exc} = 354 nm, a cylindrical lens (focal length: 2.5 cm) was employed and the excited region had length of ≈ 7 mm and width of ≈ 1.6 µm. For two-photon excitation (2PE) at λ_{exc} = 710 nm, the excited region had a length of ≈ 7 mm and width of ≈ 3.2 µm and for the three-photon excitation (3PE), the excited area had a length of ≈ 7 mm and width of ≈ 3.6 µm. The collected emission was analyzed by a CCD coupled spectrometer with an overall resolution better than 0.1 nm. All measurements were performed at room temperature.

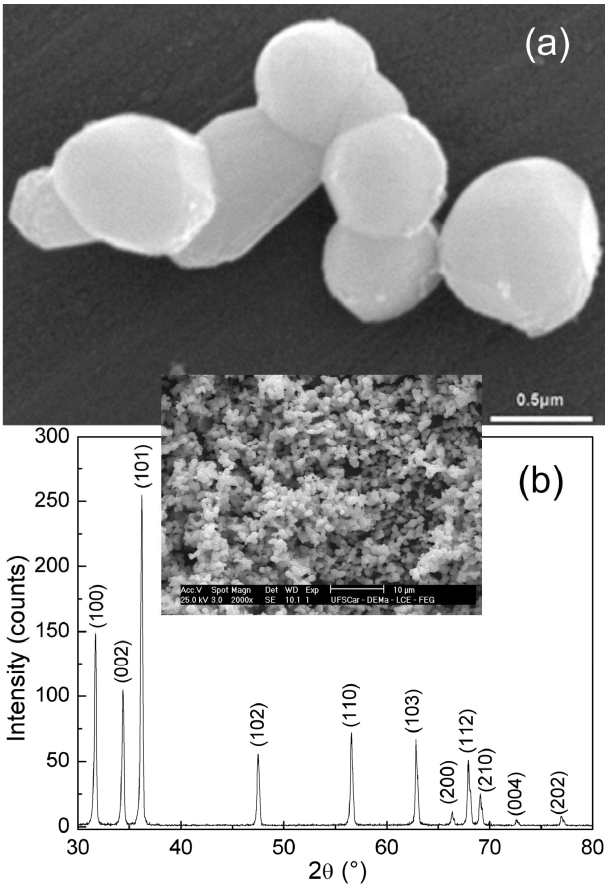

Fig. 1 (a) SEM image of ZnO grains synthesized at 1000 ºC. Grains sizes are between 500 and 700 nm. (b) X-ray diffractogram of ZnO grains. Inset: SEM image of compact ZnO powder at 1000x magnification.

Results and discussion

ZnO powders synthetized by proteic sol-gel, in addition to optimal optical properties, present a homogeneous size distribution and quasi-spherical morphology of grains,[45] standing as excellent structures for use in RL.

In the present paper we first report RL emission due to 1PE and 2PE, The results followed the same behavior as already reported in the literature[1,27,28,40] except that in the 2PE case we observed a RL spiky spectrum demonstrating for the first time the contribution of coherent feedback in quasi-spherical ZnO grains. The agreement with the previous results indicates the good quality of the ZnO grains synthesized by the new method. Fig. 2a shows the RL emitted intensity for 1PE (λ_{exc} = 354 nm), versus the excitation pulse energy (EPE). The threshold value of 0.54 µJ was obtained; the inset shows the stripe excitation geometry and an emission spectrum for excitation when the EPE is 0.47 µJ at 1KHz.

In Fig. 2b, the bandwidth reduction as a function of the EPE is shown, where one can clearly see the bandwidth narrowing down to ≈ 6 nm. The inset shows a typical single-shot spectrum obtained for EPE of 1.1 µJ, above the RL threshold. Notice that spikes due to coherent feedback are observed.

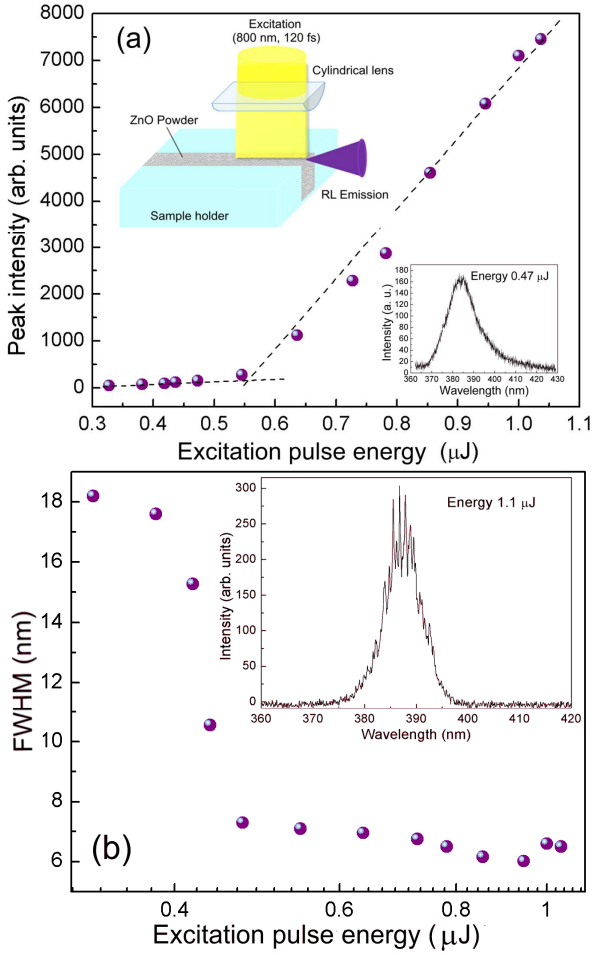

Fig. 2 One-photon ZnO RL characteristics: (a) peak intensity versus excitation pulse energy, EPE (the insets show the experimental setup and the emission spectrum for excitation below the threshold); (b) linewidth reduction versus the EPE. The inset shows a typical spectrum for EPE above threshold.

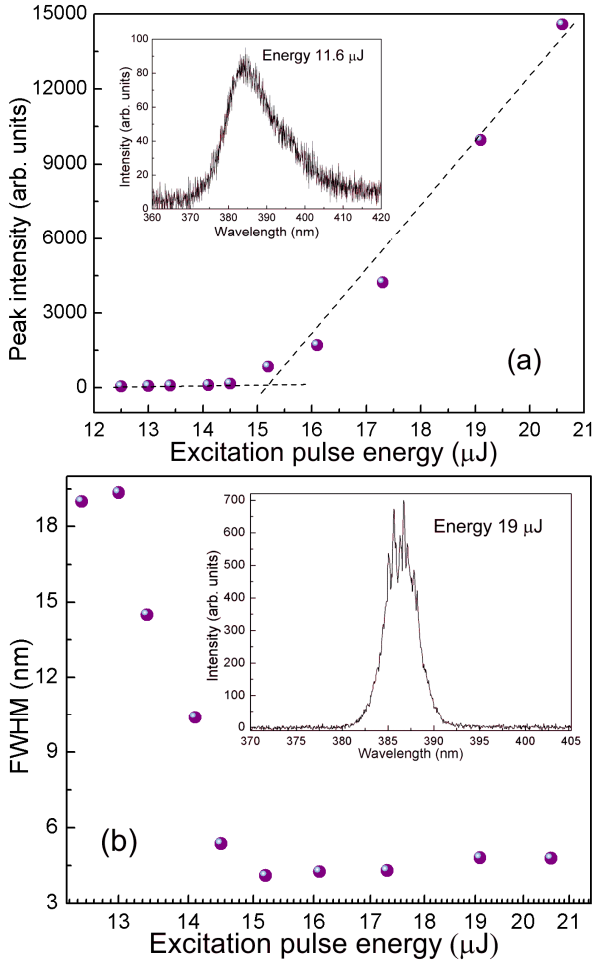

Fig. 3 Two-photon ZnO excited RL characteristics: (a) peak intensity versus the excitation pulse energy (the inset shows an emission spectrum below the threshold); (b) linewidth reduction versus excitation pulse energy. The inset shows a typical spectrum for excitation energy above threshold.

Similarly, Fig. 3 shows the RL characteristics for 2PE at λ_{exc} = 710 nm. Fig. 3a shows the RL emitted intensity versus the EPE, and Figure 3b shows the bandwidth reduction versus the EPE. In this case, the threshold inferred from Fig. 3a is ≈15 μJ, whereas the bandwidth is narrowed to about 4 nm. The inset in Fig. 3a is a single-shot emitted spectrum for EPE below threshold (11.6 μJ); no spikes are observed. The inset in Fig. 3b shows similar single-shot spectral behavior for EPE of 19 μJ, above the threshold as in the 1PE case, again confirming the coherent feedback mechanism.

The data shown in Fig.2 and Fig.3 were presented in order to compare with previous works.[15,16,40] The RL characteristics observed corroborates the quality of our samples with respect to other samples prepared by conventional methods. However, to the best of our knowledge, a new result was the demonstration of coherent feedback in the 2PE case that was not reported before. The emitted spectrum for excitation below the threshold in both cases showed a single band centered at the 387 nm.

An interesting spectral behavior appeared upon excitation at λ_{exc} = 802 nm, as shown in the luminescence spectra of Fig. 4, where two bands are present: a UV band centered at ≈ 390 nm and a violet band centered at ≈ 401 nm. According to Özgür et al.,[33] we assigned the UV band to direct conduction-to-valence band decay, which was observed only upon direct 3PE.

It is worth mentioning that similar finding was recently reported by our group using a ZnO-on-Si nanostructured film.[31] The violet band centered at ≈ 401 nm can be assigned to either second-harmonic generation (SHG) or multiphoton-absorption-induced luminescence.[46-48] As shown by Dominguez et al.,[31] we verified that the violet emission is mainly due to SHG for low EPE (below 37 μJ) and coexists with multiphoton-induced luminescence at energies higher than 37 μJ. We confirmed that the emission at 401 nm is indeed SHG, since by exciting the sample at 710 nm, the 401 nm band was no longer present but an emission at 355 nm was observed. Even though the two bands centered at 390 nm and 401 nm are adjacent, we assumed Gaussian profiles for both bands to infer the FWHM for each of them, as indicated in the caption of Fig. 4. A study of the intensity dependence of the violet and the UV bands as a function of the EPE, whose results are shown in Fig. 5a and 5b, helps to clarify the mechanisms involved. It is well known that, in the absence of saturation, the upconversion (UC) intensity, I_{UC}, is proportional to $(I_E)^n$, where n indicates the number of photons absorbed in the excitation process and I_E is the excitation intensity. Therefore, from Fig. 5a, which shows a slope corresponding to n ≈ 2, one concludes that the coexisting SHG and two-photon absorption at an interstitial Zn energy level are responsible for the violet luminescence. More detailed study about the SHG and multiphoton absorption in ZnO bulk and nanocrystals under visible and IR

femtosecond excitation can be found in earlier reports.[46-50] On the other hand, for the UV emission, the slope of n ≈ 3.5 for low EPE corroborates the assumption of a direct band-to-band three-photon absorption process. For EPE larger than 45 μJ the data shown in Fig. 5b is highly nonlinear with slope ≈ 12. The deviation of slope 3 beyond the measurement uncertainty is probably influenced by the onset of stimulated amplified emission before the feedback due to scattering leads to lasing.

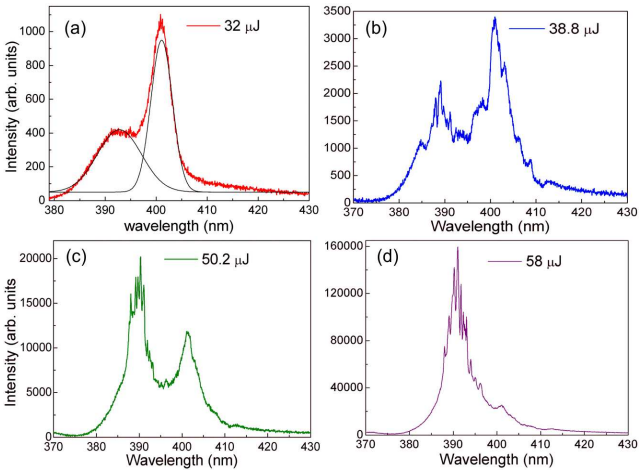

Fig. 4 (a)-(d) Emission spectra of ZnO powder in the UV- violet region for different excitation pulse energies. Solid black lines in (a) represent two Gaussian curves adjusted to the UV and violet bands, in order to determine their FWHM.

The behavior of the violet and UV bands in the present experiments is illustrated in Fig. 6a which shows two spectra at low (28.8 μJ) and high (63 μJ) EPE. It can be clearly seen the double spectral bands in both cases, but they are both smooth for low EPE and at high energy the UV band is spiky. This behavior indicates that the feedback mechanism for RL emission is the light scattering by the submicron sized particles. To confirm the RL behavior, we performed studies of the emitted intensity and linewidth spectral reduction as a function of incident energy specifically for the UV band, as shown in Fig. 6b and 6c.

To determine the RL threshold, we first note that the data shown in Fig 5b when plotted in a linear-linear graph (Fig. 6b) cannot show clearly the two inflexion points at ≈36 μJ and ≈ 48 μJ shown in Fig. 5b. Therefore we plotted the same data in an enlarged graph shown in the inset of Fig.6b and then we determined the RL threshold at 36.5 μJ.

In order to understand the lasing behavior, we consider three possible mechanisms: (i) laser emission associated to longitudinal modes of Fabry-Perot (FP) cavities formed by two opposite facets of the ZnO particles, (ii) whispering gallery modes (WGM) lasing, consequence of the total internal reflection of light inside a single particle, and (iii) random lasing due to multiple light scattering in the random media. In case (i), the separation between two adjacent longitudinal modes would be $\Delta\lambda = \lambda^2/2n_rL$ where λ is the resonant wavelength, n_r is the refractive index and L is the FP cavity length. For ZnO grains having typical dimensions of ≈ 600 nm and $n_r = 2.45$ at 390 nm, the spacing between two adjacent modes is ≈50 nm. Then, only one mode would exist in the range from 380 to 420 nm if the FP cavities formed by two-end facets of ZnO particles were responsible for the lasing effect. Consequently, we rule out the laser action due to FP cavities since a multimode characteristic was recorded. On the other hand, we recall that WGM cannot be excited in sub-micrometric particles. Since the separation between two adjacent peaks in Fig. 4c and 4d is ≈ 0.8 nm and this would be compatible with particles having diameters of ≈ 2 μm.

Therefore, the only possible mechanism for coherent laser emission is the multiple scattering of light in the random media.

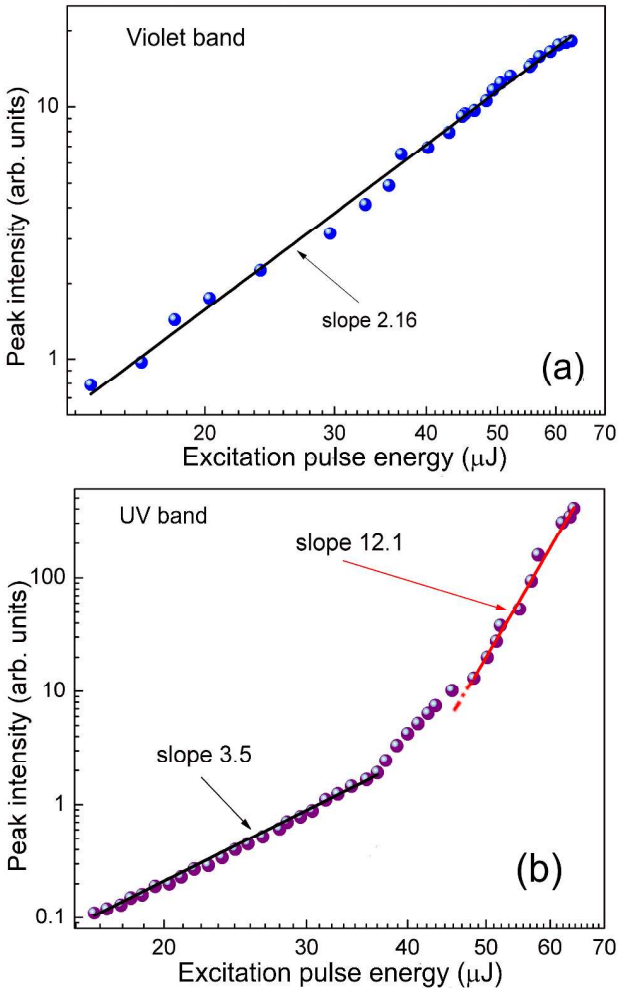

Fig. 5 Peak intensities of the UV and violet bands versus the excitation pulse energy. The dots are experimental data and the lines represent numerical fits.

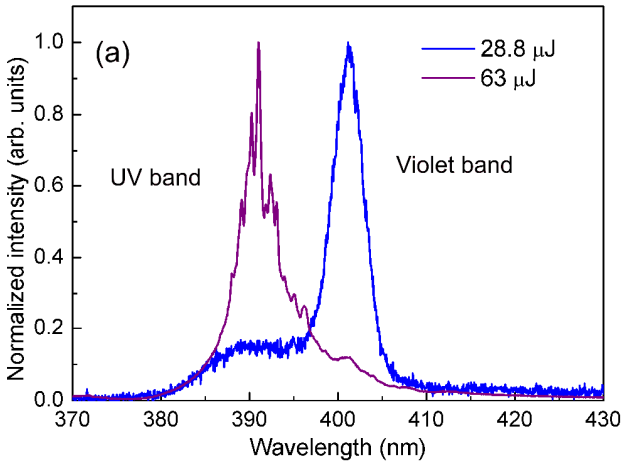

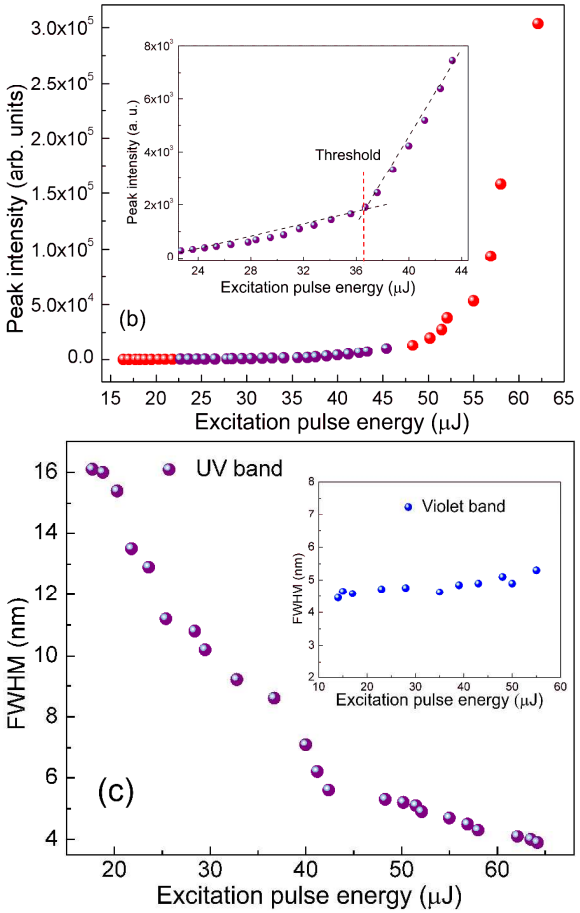

Fig. 6 (a) Spectral signature at low (28.8 μJ) and high (63 μJ) excitation pulse energy. (b) Peak intensity behavior of the emission centered at 389 nm versus the excitation pulse energy. The inset shows the threshold at 36.5 μJ. (c) Linewidth behavior of the UV band, showing the RL minimum bandwidth. The inset shows that the violet bandwidth remains essentially constant, with a slight broadening.

Two possibilities are usually considered to explain the presence of spikes in the RL spectrum. One possibility occurs in the Ioffe-Regel regime, when the mean free path is close or smaller than the laser wavelength, λ, and the disorder parameter $kl_t \leq 1$, where $k = 2\pi/\lambda$ and l_t is the transport mean free path.[1,2] Alternatively, coherent output can be due to extended modes,[2,51] in a process that does not require interference effects nor localized modes. We recall that Mujumdar et al. demonstrated the contribution of coherent feedback for kl_t ranging from 35 to 5800.[51]

As illustrated in Fig. 6a the emitted spectrum in the RL regime showed several spikes (linewidth ≈ 0.3 nm) evidencing coherent feedback; the spiky curve in the left side was obtained for excitation energy of 63 μJ while the smooth curve in the right side corresponds to a excitation pulse energy of 28.8 μJ, below the RL threshold. Considering the ZnO grains as spheres with diameter of 600 nm, the scattering cross-sections as calculated from Mie theory is 0.52 μm^2 at 390 nm. The transport mean free path, l_t, and the disorder parameter kl_t were estimated to be ≈ 515 nm and ≈ 8, respectively. Therefore, our anti-Stokes RL is operating in the strong scattering regime, close to the Ioffe-Regel regime ($l_t \sim \lambda$), and the emitted spikes are due to the strong light confinement provided by ZnO particles enhanced by the stripe excitation geometry.

Finally we comment that the increase in the RL threshold for 2PE and 3PE when compared with 1PE case is a consequence of the low efficiency of nonlinear optical absorption processes.

Conclusions

In summary, we demonstrated coherent random laser action in the strong scattering regime and close to the Ioffe-Regel regime induced by simultaneous three-photon absorption in ZnO powders. To our knowledge, this is the first demonstration of UV coherent random lasing excited by two and three-photon absorption in a semiconductor powder where the amplifying medium and scatterers are the same particles. One advantage of the multiphoton excitation scheme to obtain random lasing in the ultraviolet is that a high-frequency excitation laser is not required. Our results open new windows for the potential application of random lasers in speckle-free imaging[52] using ultraviolet illumination, biomedical imaging[53] as well as its use in the antibacterial context and photodynamic therapy.[35]

Acknowledgements

We acknowledge financial support from the Brazilian agencies Conselho Nacional de Desenvolvimento Cientifico e Tecnológico (CNPq) and the Fundação de Amparo à Ciência e Tecnologia do Estado de Pernambuco (FACEPE). The work was performed in the framework of the Photonics National Institute (INCT de Fotônica) project and PRONEX/CNPq/FACEPE.

Notes and references

[a] Departamento de Física, Universidade Federal de Pernambuco, Recife-PE 50670-901, Brazil. E-mail: anderson@df.ufpe.br

[b] Departamento de Física, Universidade Federal de Sergipe, São Cristóvão-SE 49100-000, Brazil.

[c] Laboratório de Óptica Biomédica e Imagem, Universidade Federal de Pernambuco, Recife- PE 50740-530, Brazil. E-mail: christian@df.ufpe.br

1 H. Cao, *Waves Random Media*, 2003, **13**, R1.
2 D. S. Wiersma, *Nature Phys*., 2008, **4**, 359.
3 R. V. Ambartsumyan, N. G. Basov, P. G. Kryukov and V. S. Letokhov, *IEEE J. Quant. Electron.*, 1966, **2**, 442.
4 N. M. Lawandy, R. M. Balachandran, A. S. L. Gomes and E. Sauvain, *Nature (London),* 1994, **368**, 436.
5 M. A. Noginov, *Solid State Random Lasers*, Springer, New York, 2005.
6 D. S. Wiersma, *Nature Photon.,* 2013, **7**, 188.
7 K. L. van der Molen, A. P. Mosk and A. Lagendijk, *Opt. Commun.*, 2007, **278**, 110.
8 J. U. Kang and J. B. Khurgin, *Appl. Phys. Lett.*, 2006, **89**, 221112.
9 A. Tulek, R. C. Polson and Z. V. Vardeny, *Nature Phys.*, 2010, **6**, 303.
10 M. Notomi, H. Suzuki, T. Tamamura and K. Edagawa, *Phys. Rev. Lett.*, 2004, **92**, 123906.
11 C. T. Dominguez, Yvon Lacroute, D. Chaumont, M. Sacilotti, C. B. de Araújo and A. S. L. Gomes, *Opt. Express*, 2012, **20**, 17380.
12 Q. Baudouin, N. Mercadier, V. Guarrera, W. Guerin and R. Kaiser, *Nature Phys*., 2013, **9**, 356.

13 X. Ma, P. Chen, D. Li, Y. Zhang and D. Yang, *Appl. Phys. Lett.,* 2007, **91**, 251109.
14 X.-Y. Liu, C.-X. Shan, S.-P. Wang, Z.-Z. Zhang and D.-Z. Shen, *Nanoscale,* 2012, **4**, 2843.
15 H. Zhu, C.-X. Shan, J.-Y. Zhang, Z.-Z. Zhang, B.-H. Li, D.-X. Zhao, B. Yao, D.-Z. Shen, X.-W. Fan, Z.-K. Tang, X. Hou and K.-L. Choy, *Adv. Mater*., 2010, **22**, 1877.
16 Q. Qiao, C.-X. Shan, J. Zheng, H. Zhu, S.-F. Yu, B.-H. Li, Y. Jia and D.-Z. Shen, *Nanoscale,* 2013, **5**, 513.
17 H. Cao, Y. Ling, J. Y. Xu and C. Q. Cao, *Phys Rev. Lett*., 2001, **86**, 4524.
18 M. A. R. C. Alencar, A. S. L. Gomes and C. B de Araújo, *J. Opt. Soc. Am. B*, 2003, **20**, 564.
19 C. J. S. de Matos, L. de S. Menezes, A. M. Brito-Silva, M. A. M. Gámez, A. S. L. Gomes and C. B. de Araújo, *Phys. Rev. Lett.*, 2007, **99**, 153903.
20 S. K. Turitsyn, S. A. Babin, A. E. El-Taher, P. Harper, D. V. Churkin, S. I. Kablukov, J. D. Ania-Castañón, V. Karalekas and E. V. Podivilov, *Nature Photon.*, 2010, **4**, 231.
21 Z. Hu, Q. Zhang, B. Miao, Q. Fu, G. Zou, Y. Chen, Y. Luo, D. Douguo, P. Wang, H. Ming and Q. Zhang, *Phys. Rev. Lett.*, 2012, **109**, 253901.
22 M. Gagné and R. Kashiap, *Opt. Express,* 2009, **17**, 19067.
23 Q. Song, L. Liu, S. Xiao, X. Zhou, W. Wang and L. Xu, *Phys. Rev. Lett*., 2006, **96**, 033902.
24 S. Gottardo, R. Sapienza, A. Blanco and D. Wiersma, C. López, *Nature Photon*., 2008, **2**, 429.
25 N. Bachelard, J. Andreasen, S. Gigan and P. Sebbah, *Phys. Rev. Lett.*, 2012, **109**, 033903.
26 H. E. Türeci, L. Ge, S. Rotter and A. D. Stone, *Science*, 2008, **320**, 643.
27 G. Zhu, C. E Small and M. A. Noginov, *Opt. Lett*., 2008, **33**, 920.
28 E. V. Chelnokov, N. Bityurin, I. Ozerov and W. Marine, *Appl. Phys. Lett.*, 2009, **89**, 171119.
29 M. A. S. de Oliveira, C. B. de Araújo and Y. Messaddeq, *Opt. Express*, 2011, **19**, 5620.
30 A. S. L. Gomes, M. T. Carvalho, C. T. Dominguez, C. B. de Araújo and P. N. Prasad, *Opt. Express*, 2014, **22**, 14305.
31 C. T. Dominguez, M. S. Vieira, R. M. Oliveira, M. Ueda, C. B. de Araújo and A. S. L. Gomes, *J. Opt. Soc. Am. B*, 2014, **31**, 1975.
32 G. S. He, P. P. Markowicz, T.-C. Lin and P. N. Prasad, *Nature*, 2002, **415**, 767.
33 Ü. Özgür, Ya. I. Alivov, C. Liu, A. Teke, M. A. Reshchikov, S. Doğan, V. Avrutin, S.-J. Cho and H. Morkoç, *J. Appl. Phys.*, 2005, **98**, 041301.
34 A. Janotti and C. G Van de Walle, *Rep. Prog. Phys*., 2009, **72**, 126501.
35 D. Sharma, J. Rajput, B. S. Kaith, M. Kaur and S. Sharma, *Thin Solid Films*, 2010, **519**, 1224.
36 J. Fallert, R. J. B. Dietz, H. Zhou, J. Sartor, C. Klingshirn and H. Kalt, *Phys. Status Solidi* C, 2009, **6**, 449.
37 C. Zhang, F. Zhang, T. Xia, N. Kumar, J.-I. Hahm, J. Liu, Z. L. Wang and J. Xu, *Opt. Express*, 2009, **17**, 7893.
38 C.-H. Lu, T.-Y. Chao, Y.-F. Chiu, S.-Y. Tseng and H.-C. Hsu, *Nanoscale Res. Lett.*, 2014, **9**, 178.
39 J. Fallert, F. Stelzl, H. Zhou, A. Reiser, K. Thonke, R. Sauer, C. Klingshirn and H. Kalt, *Opt. Express*, 2008, **16**, 1125.
40 H. Cao, Y. G. Zhao, S. T. Ho, E. W. Seelig, Q. H. Wang and R. P. H. Chang, *Phys. Rev. Lett*., 1999, **82**, 2278.
41 M. A. Gomes, M. E. G. Valerio and Z. S. Macedo, *J. Nanomater*., 2011, **2011**, 1.
42 P. R. J. Montes, M. E. G. Valerio, M. A. Macedo, F. Cunha and J. M. Sazaki, *Microelectr. J.*, 2003, **34**, 557.
43 J. V. A. Santos, M. A. Macedo, F. Cunha and J. M. Sazaki, J. G. S. Duque, *Microelectr. J.,* 2003, **34**, 565.
44 R. S. Silva and Z. S. Macedo, *J. Therm. Anal. Calorim.*, 2011, **103**, 587.
45 M. A. Gomes, M. E. G. Valerio, J. F. Q. Rey and Z. S. Macedo, *Mater. Chem. Phys.,* 2013, **142**, 325
46 S. K. Das, M. Biswas, D. Byrne, M. Bock, E. McGlynn, M. Breusing and R. Grunwald, *J. Appl. Phys.*, 2010, **108**, 043107.
47 D. C. Dai, S. J. Xu, S. L. Shi, M. H. Xie and C. M. Che, *IEEE Photon. Technol. Lett*., 2006, **18**, 1533.
48 C. F. Zhang, Z. W. Dong, G. J. You, R. Y. Zhu, S. X. Qian, H. Deng, H. Cheng and J. C. Wang, *Appl. Phys. Lett.*, 2006, **89**, 042117.
49 J. He, Y. Qu, H. Liu, J. Mi and W. Ji, *Opt. Express*, 2005, **13**, 9235.
50 M. G. Vivas, T. Shih, T. Voos, E. Mazur and C. R. Mendonça, *Opt. Express*, 2010, **18**, 9628.
51 S. Mujumdar, M. Ricci, R. Torre and D. S. Wiersma, *Phys. Rev. Lett.*, 2004, **93**, 053903.
52 B. Redding, M. A. Choma and H. Cao, *Nature Photon*., 2012, **6**, 355.
53 J. H. Yu, J. H. Yu, S.-H. Kwon, Z. Petrášek, O. K. Park, S. W. Jun, K. Shin, M. Choi, Y. I. Park, K. Park, H. B. Na, N. Lee, D. W. Lee, J. H. Kim and P. Schwille, T. Hyeon, *Nature Mater*., 2013, **12**, 359.

